

**ATTACHMENT B: AREA OF REVIEW AND CORRECTIVE ACTION PLAN**  
**40 CFR 146.84(b)**  
**CTV VI**

**1. Document Version History**

| Version | Revision Date | File Name                | Description of Change                 |
|---------|---------------|--------------------------|---------------------------------------|
| 1       | 7/31/2024     | Att B – CTV VI AoR_CA_v1 | Original Submission                   |
| 2       | 8/26/2025     | Att B – CTV VI AoR_CA_v2 | Response to May 15, 2025 EPA Comments |

**2. Facility Information**

Facility name: CTV VI

Facility contact: Faisal Latif, Storage Development Manager  
(661) 763-6274, faisal.latif@crc.com

Location: **Claimed as PBI**

**3. Computational Modeling Approach**

The computational modeling workflow begins with the development of a three-dimensional (3D) representation of the subsurface geology. It leverages well data (bottom and surface hole location, wellbore trajectory, well logs, etc.) and two-dimensional (2D)/3D seismic data for rendering structural surfaces into a geo-cellular grid, which also includes seismic information to understand faults and flow barriers. Attributes of the grid include porosity, permeability, and facies distributions of reservoir lithologies by subzone, as well as observed fluid contacts and saturations for each fluid phase. This geologic model is often referred to as a static model, as it reflects the reservoir at a single moment. Carbon TerraVault Holdings, LLC (CTV) licenses Schlumberger Petrel, industry-standard geo-cellular modeling software, for building and maintaining static models. The static model becomes dynamic in the computational modeler with the addition of the following:

- Fluid properties such as density and viscosity for carbon dioxide (CO<sub>2</sub>), each hydrocarbon and water phase
- Liquid and gas relative permeability
- Capillary pressure data
- Proposed injection well completions, injection rates and injection pressure over the life of the project
- Field pressure history

- Fluid geochemical analysis
- Rock and fluid compressibility

All injection wells are constant-rate controlled subject to a maximum allowable injection pressure that is based on fracture gradient with a 90 percent safety factor. Additionally, for each injector, a separate single wellbore model was built using the multiphase well nodal analysis software PROSPER, developed by Petroleum Experts Ltd. PROSPER has been used extensively in CO<sub>2</sub> enhanced oil recovery (EOR) to model CO<sub>2</sub> injection wells. Simulation estimated reservoir pressure near each injector was used as an input for the well performance modeling. Nodal analysis helped design the optimal CO<sub>2</sub> injection system, including tubing size designed to handle the constant mass rate of injection per day over the life of the project. PROSPER modeling results are presented in **Appendix 4: Operational Procedures (Appendix 4)**.

Results from the computational model are used to establish the area of review (AoR), the ‘region surrounding the geologic sequestration project where underground sources of drinking water (USDWs) may be endangered by the injection activity’ (EPA 75 FR 77230). In the case of the CTV VI storage project, the AoR encompasses the maximum areal extent of the CO<sub>2</sub> plume that was defined by 0.01 CO<sub>2</sub> global mole fraction cutoff at 100 years post-injection, and pressures great enough to endanger underground sources of drinking water (USDWs) are not anticipated outside the CO<sub>2</sub> plume footprint.

### **3.1 Model Background**

Computational modeling was completed using Computer Modeling Group’s (CMG’s) Equation of State Compositional Simulator (GEM). GEM is capable of modeling EOR, chemical EOR, geomechanics, unconventional reservoirs, geochemical EOR, and carbon capture and storage. GEM can model the flow of three components (gas, oil and aqueous) and multi-phase fluids, as well as predict phase equilibrium compositions, densities, and viscosities of each phase. This simulator incorporates all the physics associated with handling of relative permeability as a function of interfacial tension (IFT), velocity, composition, and hysteresis. Computational modeling for the CO<sub>2</sub> plume used the Peng-Robinson Equation of State and the solubility of CO<sub>2</sub> in water is modeled by Henry’s Law. The Peng-Robinson Equation of State establishes the properties of CO<sub>2</sub> over the pressures and temperatures of the model. Solubility of CO<sub>2</sub> in aqueous phase was modeled by Henry’s Law as a function of pressure, temperature, and salinity.

The plume model defines the potential quantity of CO<sub>2</sub> stored and simulates lateral and vertical movement of the CO<sub>2</sub> to define the extent of the CO<sub>2</sub> plume and the pressure changes in the reservoir during and after injection which are used to define the AoR.

The simulator predicts the evolution of the CO<sub>2</sub> plume by:

- Incorporating complex reservoir geometry and wells and utilizing a full field static geological 3D characterization of the reservoir incorporating lithology, saturation, porosity, and permeability.
- Forecasting the CO<sub>2</sub> plume movement and growth by inputting the operating parameters into simulation (injection pressure and rates).

- Assessing the movement of CO<sub>2</sub> after injection ceases and allowing the plume to reach equilibrium, including pressure equilibrium and compositions in each phase.

CMG's GEM (CMG-GEM) software has been used in numerous CO<sub>2</sub> sequestration peer reviewed papers, including:

- Simulation of CO<sub>2</sub> EOR and Sequestration Processes with a Geochemical EOS Compositional Simulator (Nghiemw et al., 2004).
- Model Predictions via History Matching of CO<sub>2</sub> Plume Migration at the Sleipner Project, Norwegian North Sea (Zhang et al., 2014).
- Geomechanical Risk Mitigation for CO<sub>2</sub> Sequestration in Saline Aquifers. (Tran et al., 2009).

### 3.2 *Site Geology and Hydrology*

Claimed as PBI



Claimed as PBI



Claimed as PBI



Claimed as PBI

### 3.3 *Model Domain*

A static geological model developed with Schlumberger's Petrel software, commonly used in the petroleum industry for exploration and production, is the computational modeling input. It allows the user to incorporate seismic and well data to build reservoir models and visualize reservoir simulation results. Model domain information is summarized in **Table 3.1**.

The geo-cellular grid covers a Claimed as PBI with model dimensions of Claimed as PBI ensuring that the computational model is large enough to account for boundary condition effects. In order to capture CO<sub>2</sub> storage mechanisms and properly resolve near-injection well effects, grid refinements are used in the project area and around the seven proposed injectors. Claimed as PBI the grid cells were refined to a size of 1,056 feet by 1,056 feet. Near each injector, a 25.6-acre region was further refined such that the grid cell size was 105.6 feet by 105.6 feet. As we move farther away from the project area, the grid cell dimensions are larger, with a maximum cell size of 5,280 feet by 5,280 feet at the model edges. These grid dimensions are designed to allow for adequate resolution of plume development, injection pressure requirements, and pressure changes in the reservoir. The model grid is aligned southeast to northwest Claimed as PBI parallel to the depositional trend of the Injection Zones. Claimed as PBI

Preferential flow pathways are primarily caused by reservoir heterogeneity, especially for permeability. The current dynamic fluid flow model captures this heterogeneity by incorporating geologic property variability (facies, porosity, permeability) based on well logs. This variability is guided by realistic spatial trends (variograms) away from the wells. As a result, the model effectively captures preferential flow pathways within the reservoir.

The open-hole logs have a half-foot resolution and an average vertical cell height of 7.7 feet was used via proportional gridding over the model domain to generate grid layers as shown in **Figure 3.4**. This cell height provides the vertical resolution necessary to capture significant lithologic heterogeneity (sand versus shale), which helps to ensure accurate upscaling of log data and distribution of reservoir properties in the static model. **Figure 3.5** shows a comparison of open-hole log data and the associated upscaled logs for the Claimed as PBI well within the model boundary but just outside the AoR.

### 3.4 *Facies, Porosity and Permeability*

Wireline log data were acquired with measurements that include, but are not limited to, spontaneous potential, natural gamma ray, borehole caliper, compressional sonic, resistivity, neutron porosity, and bulk density.



Formation porosity is determined one of two ways: from bulk density using 2.65 grams per cubic centimeter (g/cc) matrix density as calibrated from core grain density and core porosity data, or from compressional sonic using 55.5 microseconds per foot ( $\mu\text{sec}/\text{ft}$ ) matrix slowness and the Wyllie time average equation. The compaction coefficient (Hilchie, 1978) was calculated using a depth-dependent shale travel time.

Log-derived permeability is determined by applying a core-based transform that uses capillary pressure porosity and permeability along with clay values from X-ray diffraction (XRD) or Fourier transformed infrared (FTIR) analysis. Volume of clay is determined by spontaneous potential and is calibrated to core data. Core data from 16 wells of similar age formations

**Claimed as PBI**

The transform and core data are illustrated in **Figure 3.7**.

Porosity and volume of clay were distributed using sequential Gaussian simulation (kriging) within the static model and permeability was populated by applying the porosity-volume of clay-permeability transform at each cell.

For modeling purposes, facies are divided into sand and shale. Shale facies are defined as having a volume of clay greater than 30 percent and sand facies as having less than or equal to 30 percent volume of clay. While additional depositional facies within the sands are potentially present, the current petrophysical dataset suggests that these sands are adequately described by a single, clay dependent permeability transform (**Figure 3.7**).

Multiple realizations of facies distributions were calculated to capture the possible range of uncertainty. A random withholding exercise was implemented whereby 20 percent of wireline logs were randomly withheld from the model building process and compared to the property distribution from the remaining 80 percent. The base case facies distribution parameters were defined as the case with the lowest error on the withheld data population.

After facies distribution, cells with shale facies are deactivated in the simulation due to their low permeability. Within the sand facies, subfacies are handled implicitly by implementing the clay-dependent porosity-permeability transform described above. This allows sands with higher clay content to follow a lower permeability trend along a continuous transform.

Porosity and volume of clay are distributed independently within the sand facies using the same kriging parameters and methodology as the base case facies distribution. Permeability is calculated at each cell using the independently distributed porosity and volume of clay values.

**Figures 3.8(a) and 3.8(b)** show the porosity and permeability histograms for **Claimed as PBI** Injection Zones. **Figure 3.9** shows the distribution of permeability and porosity in the static model.

### **3.5 Constitutive Relationships and Other Rock Properties**

As no site-specific **Claimed as PBI** Injection Zones relative permeability data were available, data obtained from cores **Claimed as PBI**

which has a similar geologic age and depositional setting, were used for the computational simulation. Two samples from **Claimed as PBI** were used to normalize, average, and denormalize the relative permeability (see **Figure 3.6** for well location). The gas-water relative permeability Corey model was used to match the laboratory data (e.g., Honarpour et al., 1986).

Gas-water Corey model Gas:

$$k_{rgw}(S_g) = k_{rgwc} \left( \frac{S_g - S_{gc}}{1 - S_{wr} - S_{gc}} \right)^{n_g} \quad (1)$$

where  $S_g$  = current gas saturation  
 $S_{gc}$  = critical gas saturation to water displacement, 0.05  
 $k_{rgwc}$  = maximum gas relative permeability to water displacement, 0.32  
 $n_g$  = gas relative permeability curvature to water displacement, 2.55

Gas-water Corey model Water:

$$k_{rwg}(S_w) = k_{rwgc} \left( \frac{S_w - S_{wr}}{1 - S_{wr} - S_{gc}} \right)^{n_w} \quad (2)$$

where  $S_w$  = current water saturation  
 $S_{wr}$  = residual water saturation to gas displacement, 0.54, scale up to 0.25 during dynamic modeling  
 $k_{rwgc}$  = maximum water relative permeability to gas displacement, 0.447  
 $n_w$  = water relative permeability curvature to gas displacement, 3.10

Capillary pressure data were obtained from **Claimed as PBI** which is located close to **Claimed as PBI** (see **Figure 3.6** for well locations). Two samples from the **Claimed as PBI** were tested by centrifuge using an air-brine system. Laboratory-tested capillary pressure was converted to reservoir conditions and normalized by the Leverett J-function methodology (Leverett, 1941). Leverett's method creates a dimensionless function which normalizes the capillary pressure curves from different rock types and removes the effect of porosity and permeability in effort to understand the behavior of the underlying pore structure. A single capillary pressure curve was then generated based on the average permeability and porosity.

As described in Section 3.4, there are two facies defined in the model: sand and shale, with shale facies being deactivated in the simulation. Therefore, only one set of relative permeability and capillary pressure curves was used. **Figures 3.10** shows the relative permeability curves used in the Base Case and sensitivity cases (Base Case, Case G, and Case H). **Figure 3.11** shows the capillary pressure curve used in the computational model.

During pre-operational tests, additional cores will be collected, more special core analysis will be acquired, and the model will be updated accordingly. Additionally, as discussed below, several

sensitivity analyses have been conducted to investigate the uncertainty related to these parameters.

### 3.6 Mineralization

Previous studies into reactive transport modeling and geochemical reaction in CCS have shown that the amount of CO<sub>2</sub> trapped by mineralization reactions is extremely small over a 100-year post injection time frame (IPCC, 2005) for sandstone reservoirs. For the sake of computational efficiency and the minor expected effect on the AoR, reactive transport was not included as a part of the compositional simulation modeling.

Potential geochemical reactions of the Injection Zones, Confining Zone, and formation fluids with the injectate streams being considered were modeled using PHREEQC (ph-REdox-Equilibrium), the U.S. Geological Survey (USGS) geochemical modeling software. Details on the modeling procedure and results are provided in **Appendix 3: CTV VI Geochemical modeling (Appendix 3)**. The modeling indicates, as expected, that as the formations are stable quartz and Feldspar dominated mineralogy, the effect of geochemical reactions with the injectate will be minor. Based on molar mass, there is a minimal net molar mass change: 2 to 6.8 percent in the Injection Zones. This is not expected to have a major impact on porosity or permeability in the Injection Zones or the Confining Zone.

### 3.7 Boundary Conditions

The following boundary conditions were applied to the model domain:

- The Injection Formations are bound above by **Claimed as PBI** over the model domain, has low permeability, and has been shown to be a proven hydrocarbon seal **Claimed as PBI** and was thus set as a no-flow boundary.
- **Claimed as PBI** bounding conditions to the model are open, as no significant faults or stratigraphic barriers exist. The southeast and northeast boundaries were modeled with a pore volume multiplier based on regional sand and porosity mapping. The northwest boundary was modeled using a **Claimed as PBI** aquifer; aquifer properties are given in **Table 3.2**.
- The southwest boundary is set as a no-flow boundary due to the stratigraphic pinchout, thinning, and faulting associated with the uplift on the western margin.

### 3.8 Initial Conditions

Initial model conditions (start of CO<sub>2</sub> injection) of **Claimed as PBI** Injection Zones are given in **Table 3.3**, including temperature, pressure, and salinity, along with their data sources. The temperature is set as variable with depth using a fixed surface temperature of 72.5°F and a geothermal gradient of 0.012°F per foot, which was approximated from 248 logging run bottom-hole temperature recordings in and around the project area

(Figure 3.12(a)). A fixed surface temperature of 72.5°F was selected because it produced the best-fit line through the upper range of the bottom-hole temperature (BHT) data. Since BHT data from a single logging run must be corrected for circulation time the temperature gradient was aligned with the high side of the data (Bassiouni, 1994). The initial reservoir pressure was determined to be above hydrostatic with a pressure gradient of roughly 0.439 pounds per square inch per foot (psi/ft), which was approximated from RFT log data (Figure 3.12(b)). Salinity of 20,700 parts per million (ppm) was used for [REDACTED] and a salinity of 21,100 ppm was used for [REDACTED] which was approximated from water analysis in the area as discussed in Section 2.8.2 of Attachment A.

### 3.9 Operational Information

Details on the injection operation are presented in Table 3.4. The anticipated injection temperature at the wellhead is 90°F. Injection wells were assumed to be perforated throughout the entire thickness of the injection zone being targeted. Further details are provided in Attachment A and Appendix 4.

Table 3.4 includes injector locations, injection rate, anticipated perforated interval, duration, and injection pressure during the project life. All injection wells are constant-rate controlled subject to a maximum allowable downhole injection pressure that is based on the fracture gradient with a 90 percent safety factor. The CO<sub>2</sub> injection rate for each injector well versus time is shown in Figure 3.13. The cumulative CO<sub>2</sub> injection at each injector well versus time is shown in Figure 3.14. Bottom-hole pressure (BHP) versus time for each injector well is shown in Figure 3.15. Near injector reservoir pressure versus time for each injector well is shown in Figure 3.16.

### 3.10 Fracture Pressure and Fracture Gradient

Fracture gradient and maximum allowable downhole injection pressure values are given in Table 3.5. A fracture pressure gradient of 0.80 psi/ft is assumed for the Injection Zones. Within the project AoR, there is no site-specific fracture pressure or fracture gradient for the Injection Zones. However, several wells in the project vicinity do have fracture gradient data, either in the Injection Zones or in formations of similar age and depth. A step-rate test (SRT) was performed in [REDACTED] with a resultant fracture gradient of 0.82 psi/ft. Seven additional wells in the vicinity have formation integrity tests (FITs) or leak-off tests (LOTs) performed at similar depth ranges to the project Injection and Confining Zones. A total of 11 tests from these wells average 0.825 psi/ft from tests in the depth range of [REDACTED] true vertical depth (TVD). See Figure 2.5-5 of Attachment A for the locations of the wells. For the computational simulation modeling and well performance modeling, a fracture gradient of 0.8 psi/ft was assumed for all zones.

At this time, no fracture gradient information has been found for the Confining Zone. CTV will determine a site-specific fracture pressure for the Confining Zone as described in Attachment I: Pre-Operational Testing Plan.

CTV will ensure that the downhole injection pressure is below 90 percent of the Injection Zone fracture pressure, calculated at the top of the perforations in the injection wells (**Table 3.5**). CTV expects to operate the wells with a planned downhole injection pressure well below the maximum allowable injection pressure calculated using the fracture gradient and safety factor.

### **3.11 Time Steps**

Adaptive time-stepping control was used during the computational simulation. The time step duration was between a minimum of 0.00001 day to maximum of 31 days.

## **4. Computational Modeling Results**

### **4.1 Predictions of System Behavior**

**Figure 4.1** and **Figures 4.2(a) through 4.2(g)** show the computational modeling results and development of the CO<sub>2</sub> plume at different time steps. The plume boundary is defined by a 0.01 CO<sub>2</sub> global mole fraction cutoff at 100 years post-injection, which results in a boundary that contains 99.99 percent of the total injected CO<sub>2</sub> mass for injection. This cutoff provides confidence that the corrective action well review and potential impact to USDWs is conservative and has been appropriately evaluated. **Figures 4.2(a) through 4.2(g)** display cross sections of the plume evolution for the base case scenario at each injection well location. The average reservoir pressure in the approximate CO<sub>2</sub> plume area vs. time for **Claimed as PBI** zones are shown in **Figure 4.3(a)** and the maximum injection-induced pressure through time at the uppermost injection layer (directly below the top confining layer) is shown in **Figure 4.3(b)**.

As shown in **Figure 4.1**, the CO<sub>2</sub> extent is largely defined **Claimed as PBI** years post-injection for the different Injection Zones. The majority of the CO<sub>2</sub> injectate (74 percent) remains as supercritical CO<sub>2</sub> at the end of the simulation, with the remaining portion of the CO<sub>2</sub> dissolving in the formation brine over the simulated 100 years post-injection. **Figure 4.4** shows the cumulative storage for each of the mechanisms.

### **4.2 Model Sensitivity Analyses and Validation**

In addition to the plume modeling, CTV performed a volumetric estimate of the storage capacity of our plume footprint using U.S. Department of Energy (DOE) methodology (Goodman et al., 2011), using distributions from our geomodel for the storage reservoir and CO<sub>2</sub> properties, and storage efficiency coefficients for a deltaic sandstone reservoir using the widely applicable storage efficiency coefficients from Gorecki et al. (2009). P50 probability represents a 50 percent chance that a specific outcome will be achieved or exceeded and the P50 estimate from this volumetric approach was **Claimed as PBI** which is well over the estimate from our dynamic modeling, which gives us further confidence that our storage capacity estimate from the dynamic modeling is appropriate.

#### 4.2.1 *CO<sub>2</sub> Injectate Effect on Plume and pressure change*

As discussed in Section 7.2 of **Attachment A**, two major types of injectate compositions were considered based on the source:

- Injectate 1: A potential injectate stream composition from DAC or a pre-combustion source (such as a blue hydrogen facility that produces hydrogen using steam methane reforming process) or a post-combustion source (such as a natural gas fired power plant or steam generator). The primary impurity in the injectate is nitrogen.
- Injectate 2: A potential injectate stream composition from a biofuel capture source (such as a biodiesel plant that produces biodiesel from a biologic source feedstock) or from an oil and gas refinery. The primary impurity in the injectate is light-end hydrocarbons (methane and ethane).

The compositional simulation model developed in CMG-GEM software was run for the two simplified injectate compositions, and their results were also compared against a 100 percent CO<sub>2</sub> injectate case. The cumulative volume, rate, and injection duration for all three cases were kept the same.

The Injection Zones CO<sub>2</sub> plume for Injectate 1 and Injectate 2 is consistent with the plume outline for 100 percent CO<sub>2</sub> injectate (**Figure 4.5**), with negligible difference among the three cases. The CO<sub>2</sub> plume outline was defined by a 0.01 global CO<sub>2</sub> mole fraction cutoff at 100 years post-injection for all three cases. The 100-year post end of injection plumes for the three cases are shown in **Figure 4.5**. The wells that fall within the CO<sub>2</sub> plume are the same for all three cases.

Additionally, the average pore volume weighted reservoir pressure within the approximate plume boundary for three Injection Zones was plotted for the three cases and was found to be very close, with a maximum difference of 4 pounds per square inch (psi) seen between the cases, as shown in **Figure 4.6**. Multiple scenarios were also run to test the effect of mixing Injectate 1 and Injectate 2 in different ratios on the plume shapes. As expected, because the resulting mixed injectates were still high-purity CO<sub>2</sub> streams with impurity concentrations in between those of Injectates 1 and 2, the plume shapes for these scenarios were within the envelope represented by the end-point compositions.

In summary, there is minimal effect of the minor components on the CO<sub>2</sub> plume boundary for the proposed injectate compositions. As such, CTV's plume and AoR modeling for corrective action assessment is adequate for the expected injectate composition ranges. CTV will confirm that the properties of the injectate are consistent with the model inputs during pre-operational injectate sampling, and will do so for any additional sources. In addition, the AoR will be reviewed per Section 6, Reevaluation Schedule and Criteria.

#### 4.2.2 *Sensitivity Cases*

The base model simulation case (base case) contains a realistic representation of the hydrogeologic structure with conservative assumptions about site conditions, making the base

case suitable for delineating the AoR. A sensitivity analysis was performed to examine the effects of varying inputs that represent site conditions with the potential to significantly impact the simulation results. The sensitivity analysis scenarios are listed in **Table 4.1** and include permeability, porosity, phase trapping, relative permeability end points and shape, and capillary pressure. The sensitivity analysis is performed using 100 percent CO<sub>2</sub> injectate in all scenarios. Results from the sensitivity analysis are displayed graphically in **Figure 4.7 and 4.8**.

To quantify the results of the sensitivity analysis, the size of the CO<sub>2</sub> plume was measured as an area (using the 0.01 CO<sub>2</sub> global mole fraction cutoff at 100 years post-injection) and the changes are quantified as percentage changes compared with the base case. There are only two cases with a plume size change greater than 10 percent compared to the base case. Case C results in a +34.7 percent plume size change, corresponding to increasing the permeability transform by a multiplier of 3, which is a high-end increase in the system permeability. Case A showed a -12.1 percent plume size change, corresponding to a porosity multiplier of 1.24. In all the sensitivity cases, the resulting CO<sub>2</sub> plume boundaries are similar and do not overlie additional corrective action wells except for Case C. Case C would have the potential to add three corrective action wells within the plume.

Overall, based on these sensitivity analyses, the proposed base case is considered conservative. The sensitivity analysis provides confidence that the corrective action well review and assessment of the potential endangerment of the USDW based on the base case are conservative and have been appropriately evaluated. During pre-operational testing, the model will be updated and the AoR and corrective action wells list will be re-evaluated based on the additional site-specific data gathered.

### **4.3 AoR Delineation**

AoR delineation consists of determining the outermost extent of the separate-phase CO<sub>2</sub> plume and area of elevated pressure (pressure front) that pose risk to USDWs during the lifetime of the project. Elevated pressure may pose a risk to USDWs due to the potential for brine leakage from the injection zone into a USDW through an existing conduit, such as an improperly abandoned well. In most cases the AoR will at a minimum be defined by the CO<sub>2</sub> plume footprint and may be larger if the pressure front extends beyond the CO<sub>2</sub> plume. CTV VI used the risk-based AOR approach as documented in **Appendix 9: Risk Based AoR Delineation (Appendix 9)**.

Various methods are available to determine the pressure threshold value that defines the outermost extent of the pressure front. In general, these methods are used to define a pressure at which brine will leak upwards through an abandoned well, leak into a USDW, and endanger the USDW due to water quality impairment. Risk-based AoR delineation accounts for processes that inhibit brine leakage through abandoned wells (e.g., presence of the mud column) and processes that minimize potential USDW impacts from hypothetical brine leakage (e.g., dilution and attenuation in the USDW). Risk-based AoR delineation strategies are supported by the U.S. Environmental Protection Agency (EPA) *Class VI AoR and Corrective Action Guidance* (p. 42).



**Appendix 9** risk-based AoR delineation consisted of modeling brine leakage under conservative assumptions and resulting salinity impacts to the lowermost USDW. Brine leakage and USDW salinity transport modeling used conservative assumptions and accepted methods to simulate (1) brine leakage through an abandoned well and (2) subsequent contaminant fate and transport within the lowermost USDW. Modeling indicated that the vast majority of brine leakage through a hypothetical abandoned well in the vicinity of the project would discharge to the Claimed as PBI Monitoring Zone (below the lowermost USDW); therefore, brine leakage to the USDW would be negligible. Concomitantly, elevated salinity levels in the lowermost USDW are calculated to be negligible. These results were based on an assumed injection-zone pressure increase of 500 psi. CMG-GEM modeling results indicate that a pressure increase of this magnitude will not occur outside the boundary of the CO<sub>2</sub> plume (**Figure 4.3(b)**).

Based on these results, pressures great enough to endanger USDWs are not anticipated outside the CO<sub>2</sub> plume footprint, and the final AoR boundary was based on the extent of the CO<sub>2</sub> plume. **Figure 4.9** shows the AoR extent, injector locations, and proposed monitoring well locations. Details on the monitoring wells are discussed further in **Attachment C**.

## 5. Corrective Action

### 5.1 *Tabulation of Wells within the AoR*

Wells within the AoR are associated with Claimed as PBI. As such, there are excellent records for wells drilled in the study area and no undocumented historical wells in the AoR are expected.

CTV accessed internal databases as well as California Geologic Energy Management Division (CalGEM) information to identify and confirm wells within the AoR (California Department of Conservation, 2024; CalGEM, 2024).

**Table 5.1** provides counts of wellbores that penetrate the confining zone within the AoR by status and type, for each wellbore with a unique API-12 identifier. **Appendix 6** provides a complete list of all wellbores by API-12 within the AoR. As required by 40 CFR 146.84(c)(2), the well table in **Appendix 6** describes each well's type, construction, date drilled, location, measured depth, completion record relative to the injection zones, record of plugging, and requirement for corrective action, if necessary.

### 5.2 *Protection of USDWs*

For the project area, CTV assessed USDW protection by evaluating all wellbores that penetrate the Confining Zone in the AoR. The corrective action assessment included the generation of detailed casing diagrams for each wellbore, review of all perforations, top of cement assessment for each casing string, and determination of cement plug depths. Non-endangerment of USDWs will be ensured during all stages of the project.



### **5.3 Wells Penetrating the Confining Zone**

For wells penetrating the Confining Zone, the depth of the Confining Zone was determined by interpretation of open-hole well logs in conjunction with the deviation survey. Two wells in the AoR penetrate the Confining Zone. These wells also penetrate the Injection Zone. Both wells lie inside the CO<sub>2</sub> plume boundary and will be re-abandoned prior to injection.

### **5.4 Corrective Action Assessment of Wells in AoR**

The two wells in the AoR were drilled **Claimed as PBI**

CTV will re-abandon these wells prior to injection to ensure that confinement is reestablished. A map with these wells is shown in **Figure 5.1**, and the table of wells in **Appendix 6** provides well information pursuant to 40 CFR §146.84(c)(2). Details of the abandonment procedures for these wells are provided in **Appendix 7** and **Appendix 8**.

### **5.5 Plan for Site Access**

CTV has obtained surface access rights for the duration of the project.

### **5.6 Corrective Action Schedule**

The two wells that fall in the AoR will be re-abandoned prior to injection. CTV will ensure that CO<sub>2</sub> is confined to the injection zones within the AoR, protecting the overlying USDW and ensuring confinement.

Through time, if the plume development is not consistent with the predicted results, computational modeling will be updated to reassess the AoR. In this event, any new wells in the updated AoR will be subject to the Corrective Action Plan and will be remediated if necessary.

## **6. Reevaluation Schedule and Criteria**

### **6.1 AoR Reevaluation Cycle**

CTV will reevaluate the AoR at a minimum every five years during the injection and post-injection phases, as required by 40 CFR 146.84 (e).

Simulation study results will be reviewed when operating data is acquired. Preparation of necessary operational data for the review includes injection rates and pressures, CO<sub>2</sub> injectate concentrations, and monitoring well information (storage reservoir and overlying monitoring intervals).

Dynamic operating and monitoring data that will be incorporated into future reevaluation will include:

1. Pressure data from monitoring wells that constrain and define plume development.

2. CO<sub>2</sub> content/saturation from monitoring wells. These data may be acquired with direct aqueous measurements and cased hole log results that will constrain and define plume development.
3. Injection pressures and volumes. The injection pressures and volumes in the computational model are maximum values. If the actual rates are lower than expected, the plume will develop at a slower rate than expected and be reflected in the pressure and CO<sub>2</sub> concentration data in 1 and 2 above.
4. A review of the full suite of water quality data collected from monitoring wells in addition to CO<sub>2</sub> content/saturation to evaluate the potential for unexpected reactions between the injected fluid and the rock formation.
5. Review and submission of any geologic data acquired since the last modeling effort, including any additional site characterization performed for future injection wells.
6. Reevaluation modeling results will be compared with the most recent modeling (i.e., from the most recent AoR reevaluation). A report describing the comparison of the modeling results will be provided to EPA with a discussion on whether the results are consistent.
7. Description of the specific actions that will be taken if there are discrepancies between monitoring data and prior modeling results (e.g., remodel the AoR, update all project plans, perform additional corrective action if needed, and submit the results to EPA).

The reevaluated results will be compared to the original results to understand dynamic inputs affecting plume development and static inputs that would impact injectivity and storage capacity. Discrepancies between the initial and reevaluated models may be due to static reservoir properties such as permeability, sand continuity, and porosity or other input parameters. Although the AoR has been fully delineated, all inputs to both the static and dynamic model will be reviewed.

As needed, CTV will review all of the plans that are impacted by a potential AoR increase such as corrective action and emergency and remedial response. For corrective action, all wells potentially impacted by a changing AoR will be addressed immediately.

## **6.2 Triggers for AoR Reevaluations Prior to the Next Scheduled Reevaluation**

An ad-hoc reevaluation prior to the next scheduled reevaluation will be triggered if any of the following occur:

- Changes in pressure or injection rate that are unexpected and outside three standard deviations from the average will trigger a new evaluation of the AoR.
- Difference between the computation modeling and observed plume development:
  - ◊ Unexpected changes in fluid constituents or pressure outside the zones of injection that are not related to well integrity.
  - ◊ Reservoir pressure increase versus injected volume is inconsistent with computational modeling results with a variance  $> \pm 10$  percent from the base case simulation.

- ◊ Any other activity prompting a model recalibration.
- Seismic monitoring anomalies within 2 miles of the injection well that are indicative of:
  - ◊ The presence of faults near the Confining Zone that indicates propagation into the Confining Zone.
  - ◊ Events reasonably associated with CO<sub>2</sub> injection that are greater than M3.5.
- Exceeding 90 percent of the geologic formation fracture pressure in any injection or monitoring wells.
- Detection of changes in shallow groundwater chemistry (e.g., a significant increase in the concentration of any analytical parameter that was not anticipated by the AoR delineation modeling).
- Initiation of competing injection projects within the same injection formation within a 1-mile radius of the injection well (including when additional CTV injection wells come online).
- A significant change in injection operations, as measured by wellhead monitoring.
- Significant land-use changes that would impact site access.
- Any other activity prompting a model recalibration.

CTV will discuss any such events with the UIC Program Director as soon as possible to determine if an AoR reevaluation is required. If an unscheduled reevaluation is triggered, CTV will perform the steps described at the beginning of this section of the plan within six months for the triggering event.

## References

Claimed as PBI

[REDACTED]

[REDACTED]

[REDACTED]

[REDACTED]

[REDACTED]

[REDACTED]

[REDACTED]

Claimed as PBI

Claimed as PBI

1

1

## **Figures**

# Claimed as PBI



**Figure 3.1.** Cross section showing stratigraphy and lateral continuity of major formations across the AoR.

# Claimed as PBI



**Figure 3.2.** Location of wells with open-hole log data used to develop static and computational models.

# Claimed as PBI

A large black rectangular area representing the model boundary and geo-cellular grid. The text "Claimed as PBI" is written in large red letters at the top of this area.

**Figure 3.3.** Plan view of model boundary and geo-cellular grid used to define the CO<sub>2</sub> plume extent and associated AoR.



# Claimed as PBI



**Figure 3.4.** Static model grid layering of Injection Zone formations.

# Claimed as PBI



**Figure 3.5.** Well **Claimed as PBI** upscaled logs vs. open-hole logs.

# Claimed as PBI



**Figure 3.6.** Location of wells with core data used for permeability transform and constitutive relationships

# Claimed as PBI

**Figure 3.7.** Permeability transform for CTV VI Injection zones. **Claimed as PBI**

and are the basis for the permeability transform. Additional Core data from the Sacramento basin is also shown in green, with circles corresponding to Late Cretaceous age rock, diamonds corresponding to Paleocene age rock, and squares corresponding to Eocene age rock. The black data points are core from a well specific to the CTV VI model area. Data shown is limited to those core data points representing sand, with a clay volume from XRD of less than 25% clay and exclude any percussion sidewall derived permeability values.

# Claimed as PBI



**Figure 3.8(a).** Claimed as PBI Injection Zones porosity and permeability distribution used in static model.

# Claimed as PBI



**Figure 3.8(b).** Claimed as PBI Injection Zones porosity and permeability distribution used in static model.

# Claimed as PBI



**Figure 3.9.** Section B-B' through the static grid showing distribution of porosity and permeability in Injection and Confining Zones.

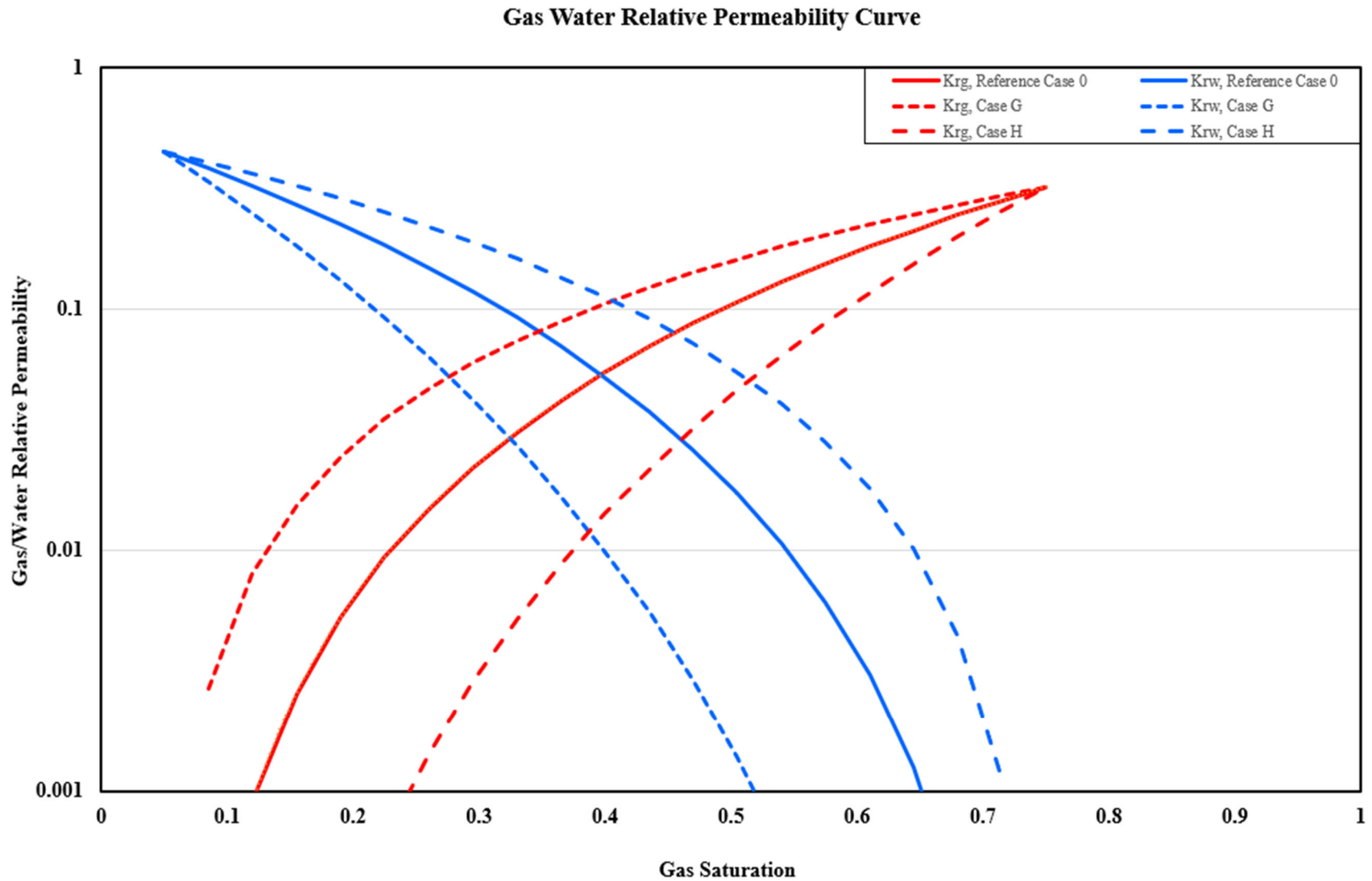


**Figure 3.10.** Relative permeability curves for Gas-Water system.



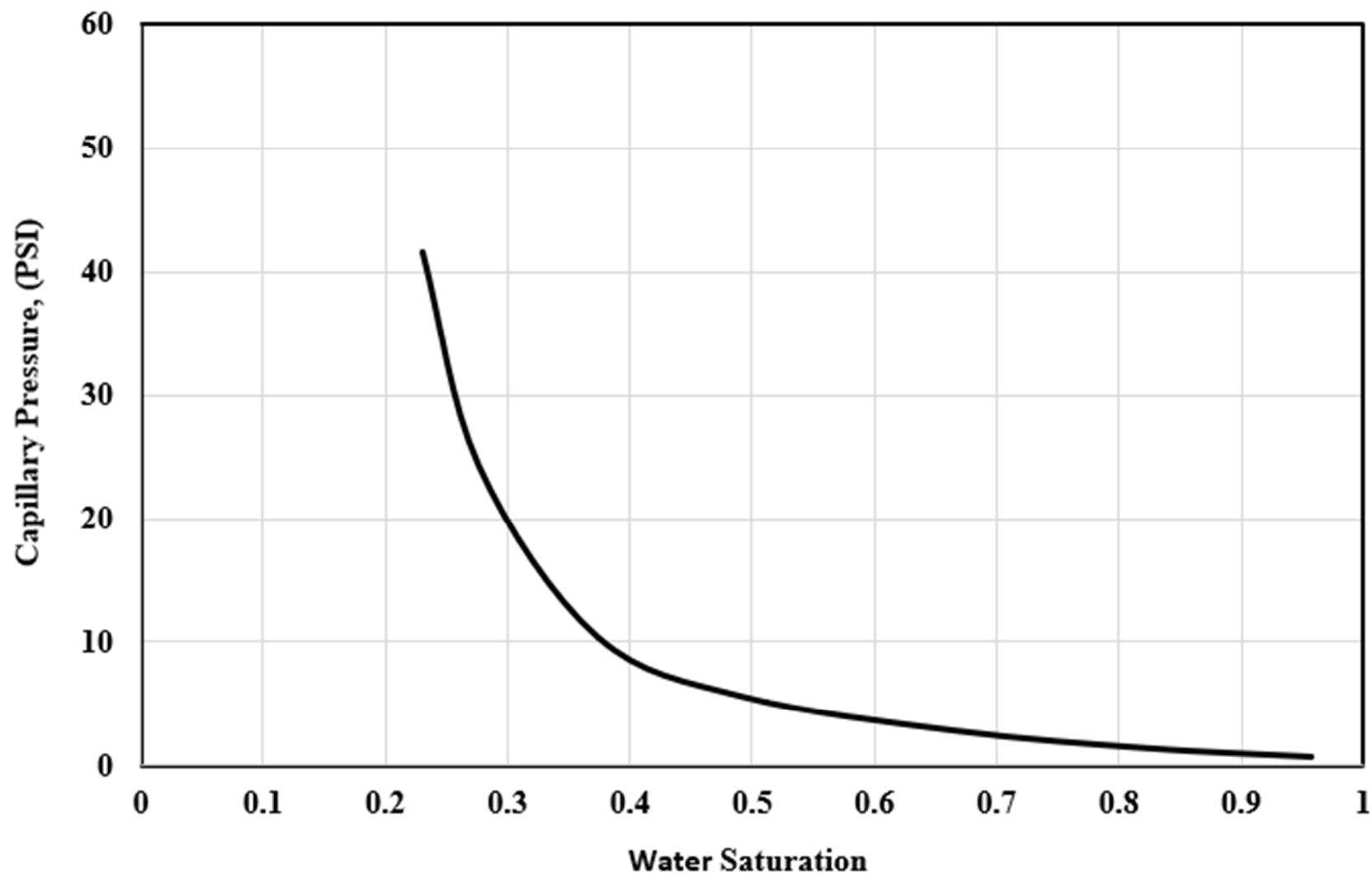


**Figure 3.11.** Capillary pressure curve.

# Claimed as PBI



**Figure 3.12(a).** Geothermal gradient used for model initial conditions. The gradient is based on 248 bottom-hole temperature datapoints from individual logging runs.

# Claimed as PBI



**Figure 3.12(b).** Well locations with RFT pressure data.

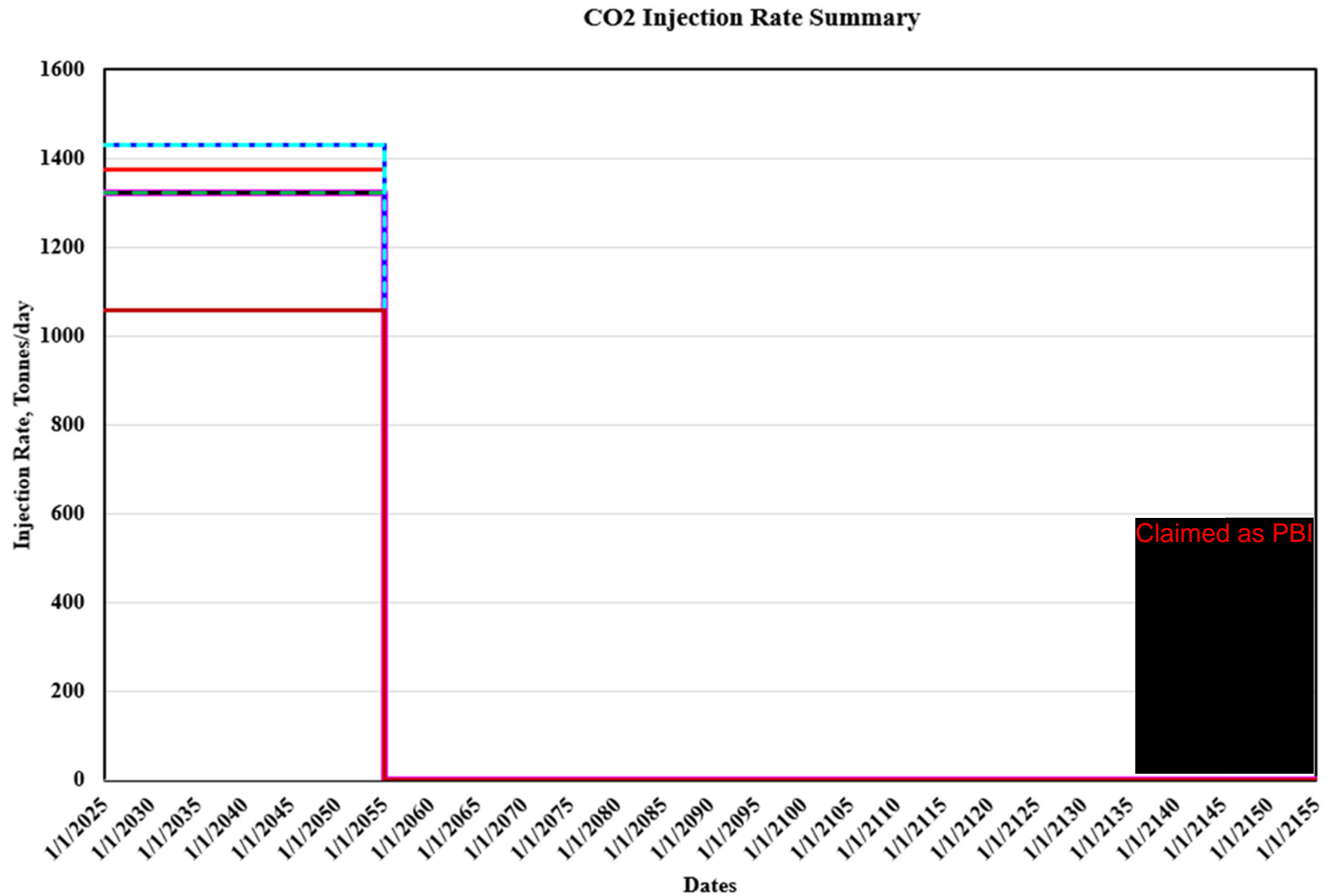


**Figure 3.13.** Base case CO<sub>2</sub> injection rate vs. time for each injector.

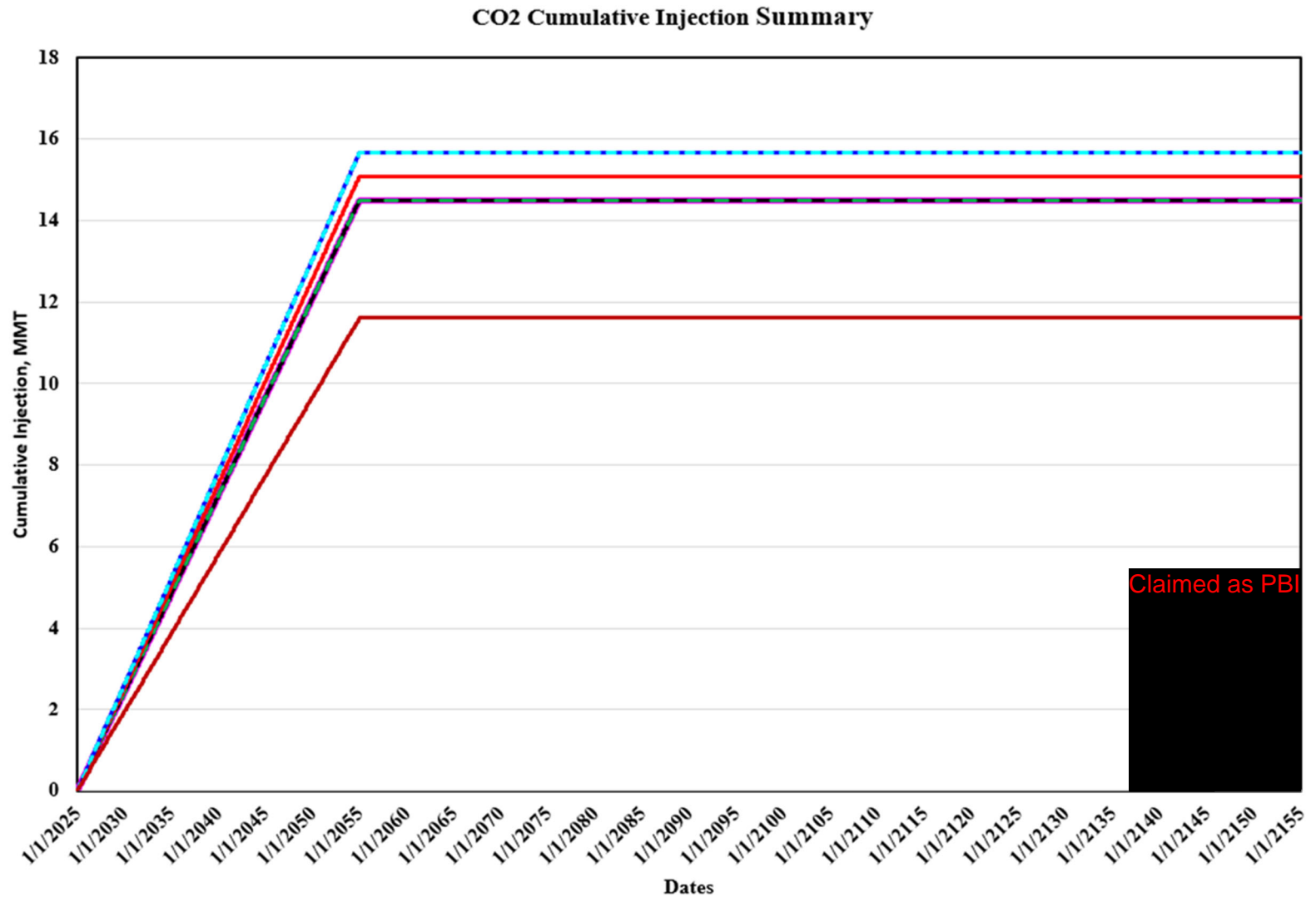


**Figure 3.14.** Base case CO<sub>2</sub> cumulative CO<sub>2</sub> injection vs. time for each injector.

## Well Bottom Hole Pressure Summary

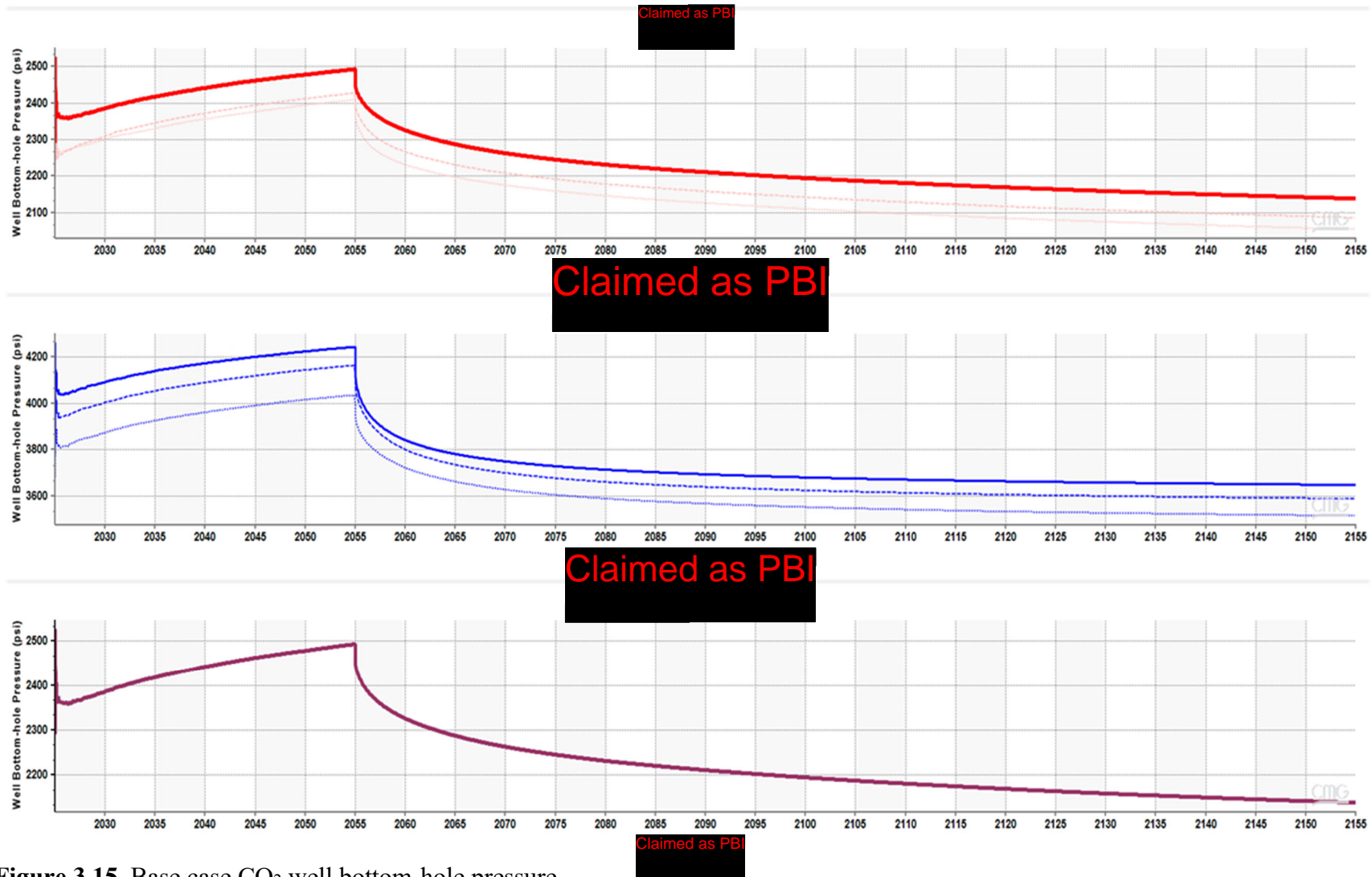


**Figure 3.15.** Base case CO<sub>2</sub> well bottom-hole pressure.

## Near Injector Reservoir Pressure Summary

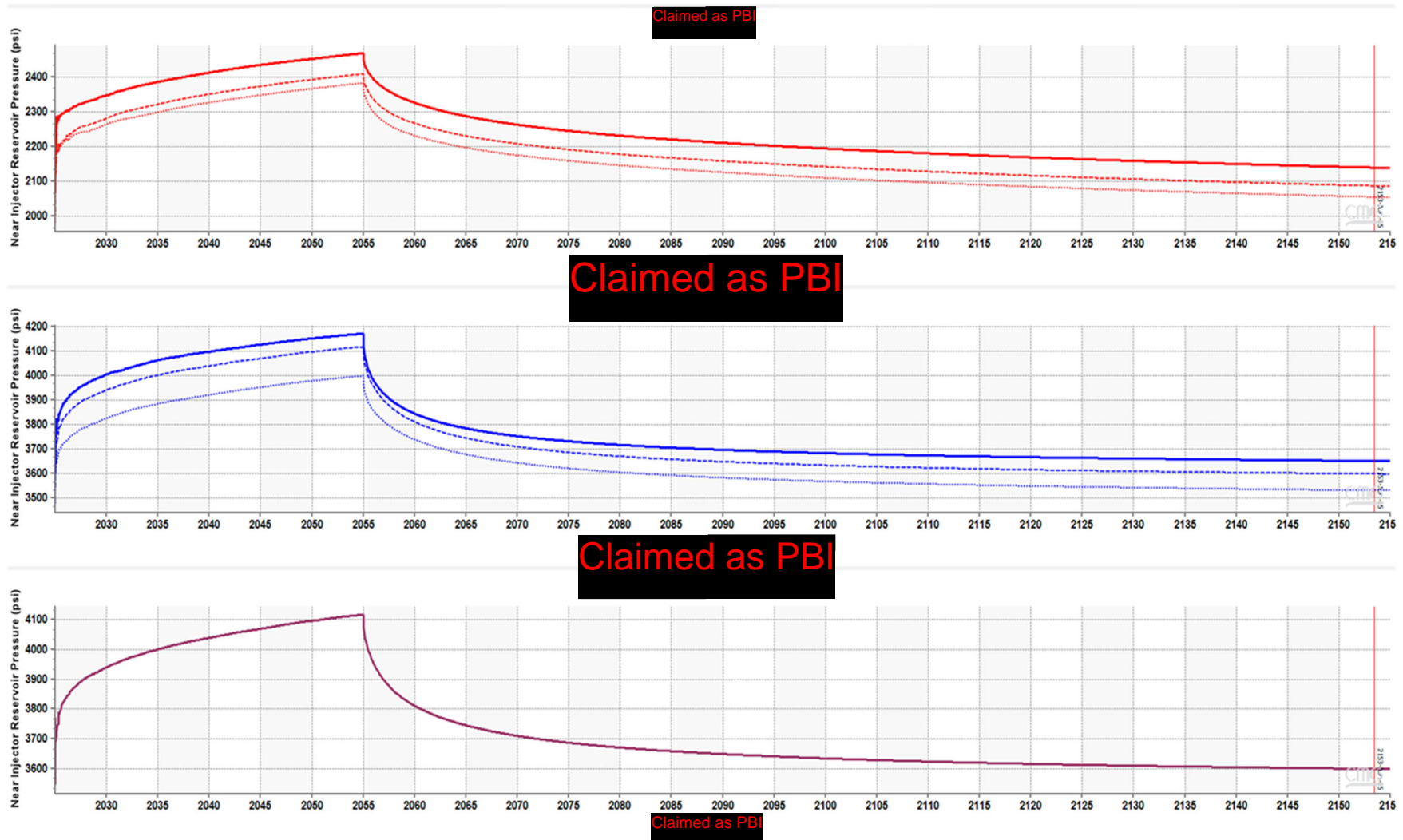


Figure 3.16. Base case CO<sub>2</sub> near injectors reservoir pressure for each injector.

# Claimed as PBI

**Figure 4.1.** Injection Zone plume development through time: 1-year, 5-year, 10-year, 30-year (end of injection), 20-year, and 100-year post-injection.



# Claimed as PBI

**Figure 4.2(a).** Base case CO<sub>2</sub> well **Claimed as PBI** CO<sub>2</sub> global mole fraction distribution at 1 year, 5 years, 10 years, 30 years (projected end of injection), 50 years (since start of injection), and 100 years post-injection.

# Claimed as PBI

**Figure 4.2(b).** Base case CO<sub>2</sub> well **Claimed as PBI** CO<sub>2</sub> global mole fraction distribution at 1 year, 5 years, 10 years, 30 years (projected end of injection), 50 years (since start of injection), and 100 years post-injection.

# Claimed as PBI

**Figure 4.2(c).** Base case CO<sub>2</sub> well **Claimed as PBI** CO<sub>2</sub> global mole fraction distribution at 1 year, 5 years, 10 years, 30 years (projected end of injection), 50 years (since start of injection), and 100 years post-injection.

# Claimed as PBI

**Figure 4.2(d).** Base case CO<sub>2</sub> well **Claimed as PBI** CO<sub>2</sub> global mole fraction distribution at 1 year, 5 years, 10 years, 30 years (projected end of injection), 50 years (since start of injection), and 100 years post-injection.

# Claimed as PBI

**Figure 4.2(e).** Base case CO<sub>2</sub> well **Claimed as PBI** CO<sub>2</sub> global mole fraction distribution at 1 year, 5 years, 10 years, 30 years (projected end of injection), 50 years (since start of injection), and 100 years post-injection.

# Claimed as PBI

**Figure 4.2(f).** Base case CO<sub>2</sub> well **Claimed as PBI** CO<sub>2</sub> global mole fraction distribution at 1 year, 5 years, 10 years, 30 years (projected end of injection), 50 years (since start of injection), and 100 years post-injection.

# Claimed as PBI

**Figure 4.2(g).** Base case CO<sub>2</sub> well **Claimed as PBI** CO<sub>2</sub> global mole fraction distribution at 1 year, 5 years, 10 years, 30 years (projected end of injection), 50 years (since start of injection), and 100 years post-injection.

## Average Reservoir Pressure in Approximate CO2 Plume Area vs. Time

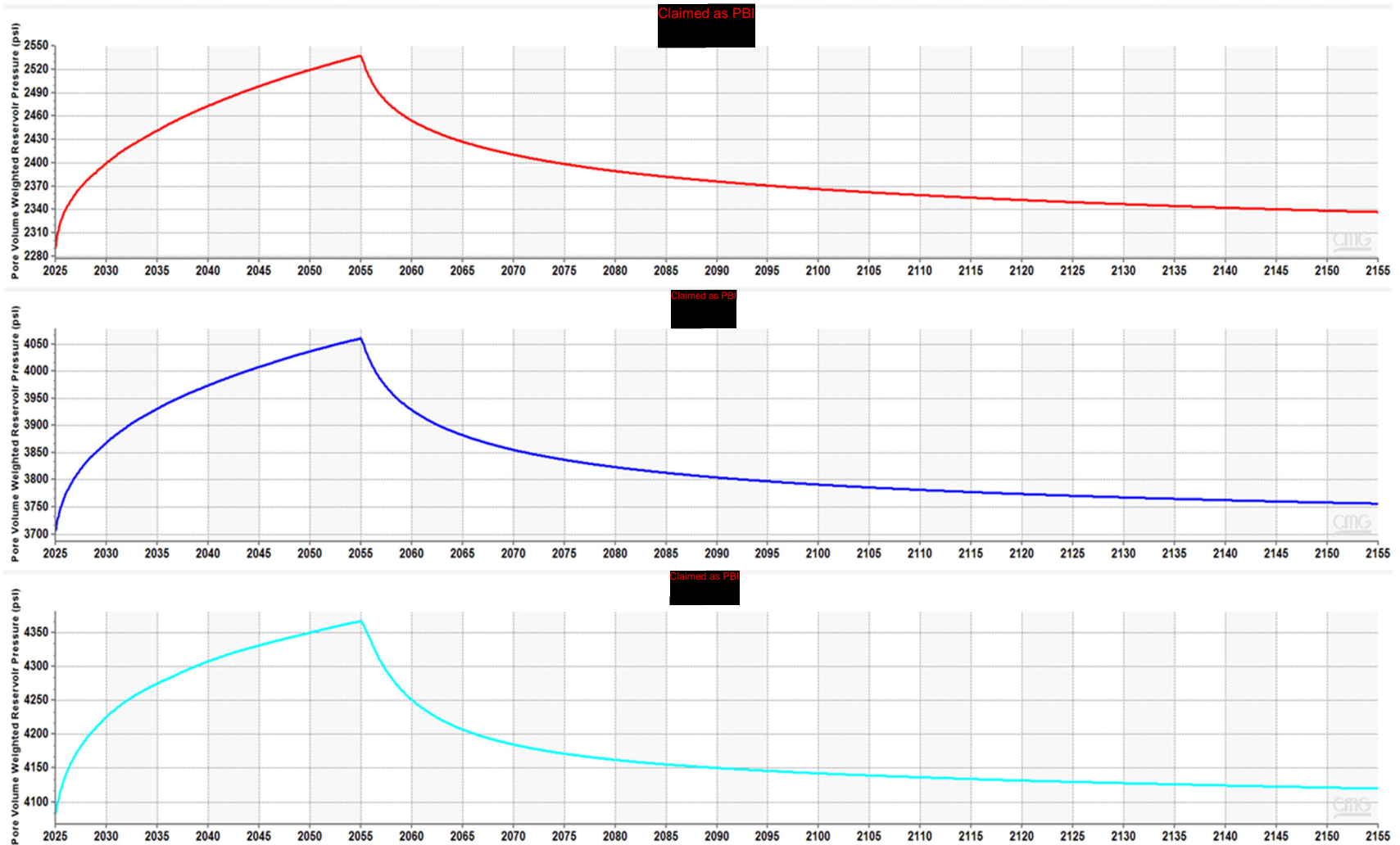


**Figure 4.3(a).** Base case CO<sub>2</sub> Average reservoir pressure within approximate plume area.



# Claimed as PBI



**Figure 4.3(b).** Maximum injection-induced pressure through time at the uppermost injection layer (directly below the top confining layer).

### Injection Zone

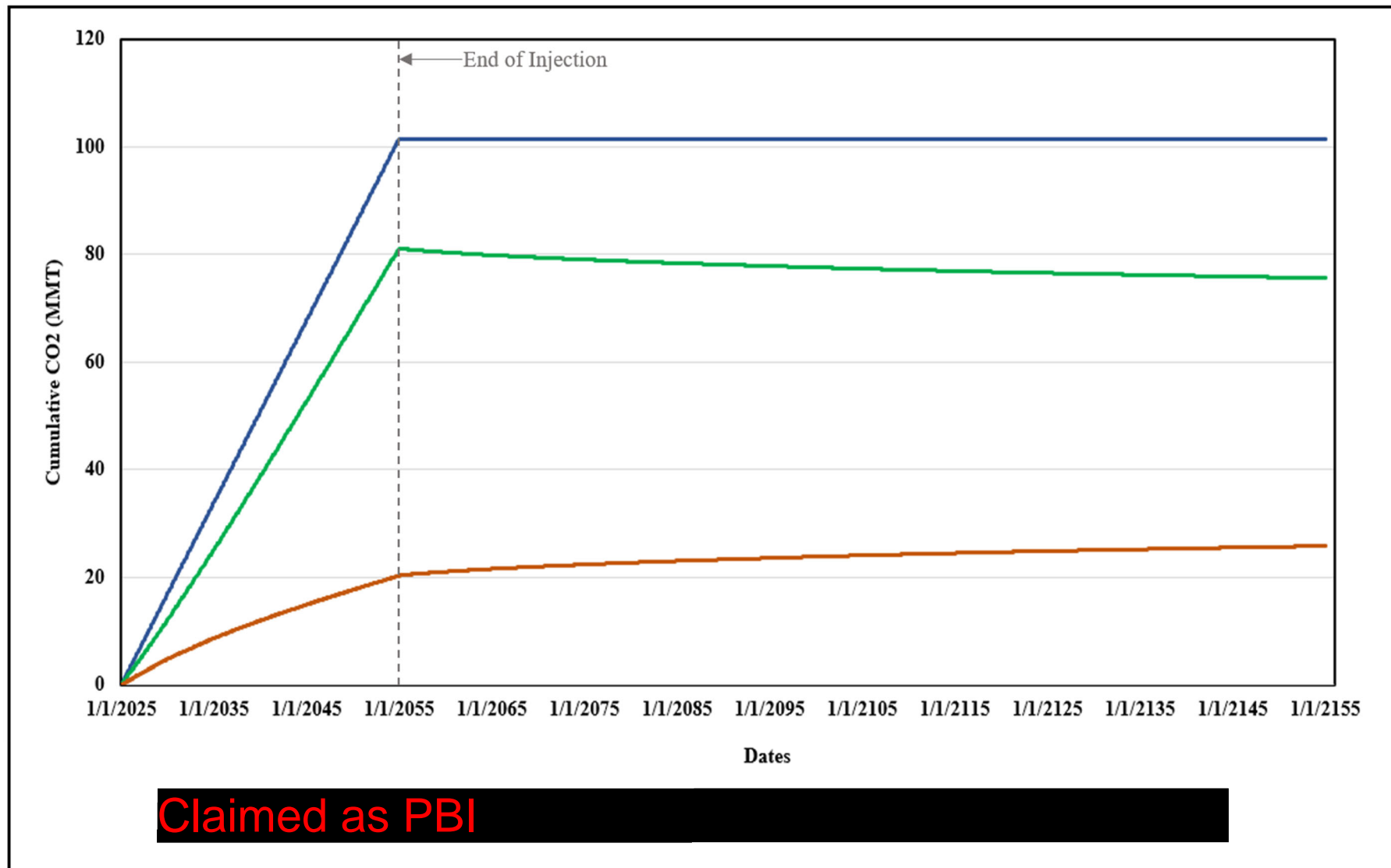


**Figure 4.4** CO<sub>2</sub> storage mechanisms in the reservoir.

# Claimed as PBI

**Figure 4.5.** CO<sub>2</sub> plume boundary for Injectate 1 case (light blue dash line), Injectate 2 case (light green dashed line), and Base case CO<sub>2</sub> (red). Larger pink outline is the model boundary. Minimal differences in plume boundaries are observed among the three cases, with boundaries generally overlying each other.

## Average Reservoir Pressure in Approximate CO<sub>2</sub> Plume Area vs. Time

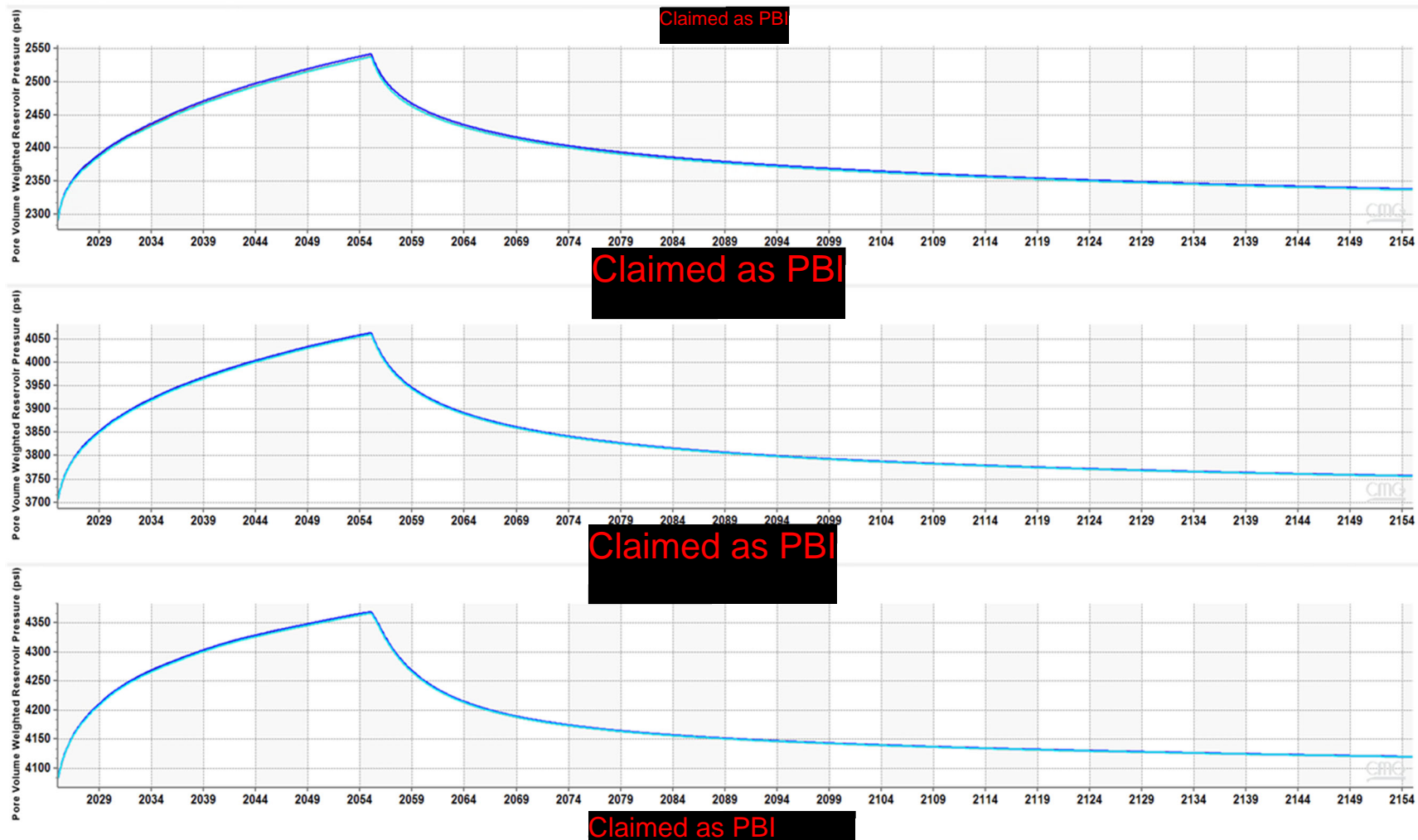


**Figure 4.6.** Average reservoir pressure within approximate plume area for Injectate 1, Injectate 2, and Base case (100% CO<sub>2</sub>). Pressure trends for all cases plot almost on top of each other.

# Claimed as PBI

**Figure 4.7.** Submitted plume boundary and CO<sub>2</sub> plume outlines for CASE A to CASE J vs. reference case (Case 0) with 100% CO<sub>2</sub>. Larger red outline is model boundary. Minimal difference in plume boundaries for most scenarios except for Case C with extreme parameters. CO<sub>2</sub> plume is defined by 0.01 CO<sub>2</sub> global mole fraction cutoff 100 years post-injection. See **Table 4.1** for scenario descriptions.

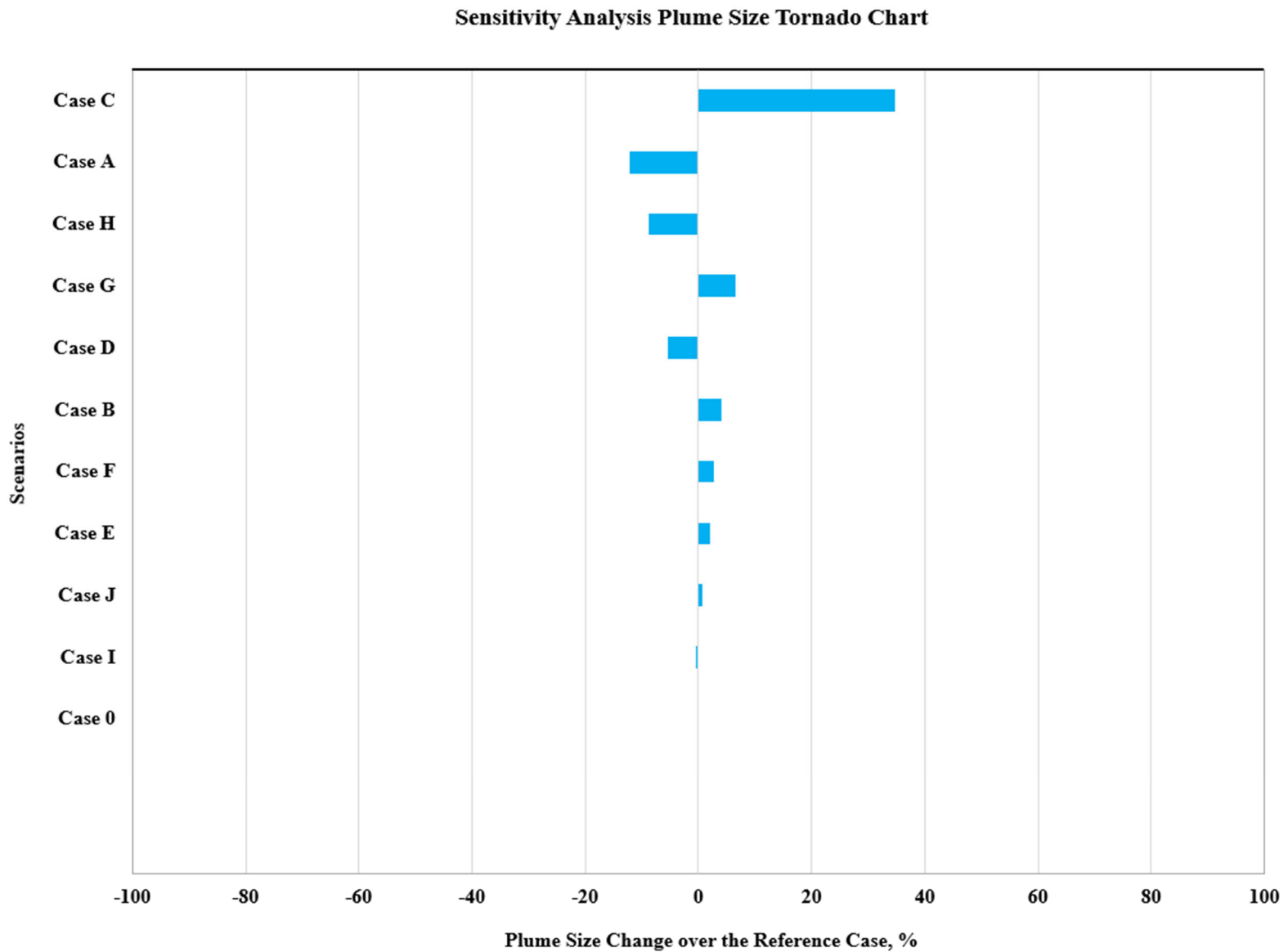


**Figure 4.8.** Injection Zone, Sensitivity analysis Tornado chart for plume size. See **Table 4.1** for scenario descriptions.

# Claimed as PBI



**Figure 4.9.** Location of injection and monitoring wells.

# Claimed as PBI



**Figure 5.1.** Wells penetrating **Claimed as PBI** confining layer within 1 mile of the AoR. Two wells are identified as falling within the AoR and for corrective action.



## **Tables**

**Table 3.1. Model Domain Information**

|                               |                               |                            |                |
|-------------------------------|-------------------------------|----------------------------|----------------|
| Coordinate System             | State Plane                   |                            |                |
| Horizontal Datum              | North American Datum (NAD) 27 |                            |                |
| Coordinate System Units       | Feet                          |                            |                |
| Zone                          | Zone 2                        |                            |                |
| FIPSZONE                      | 0402                          | ADSZONE                    | 3301           |
| Coordinate of X min           | Claimed as PBI                | Coordinate of X max        | Claimed as PBI |
| Coordinate of Y min           | Claimed as PBI                | Coordinate of Y max        | Claimed as PBI |
| Elevation of Bottom of Domain | Claimed as PBI                | Elevation of Top of Domain | Claimed        |

**Table 3.2.** **Claimed as PBI** Aquifer Property

Claimed as PBI

**Table 3.3. Initial Conditions**

| Parameter          | Injection Zone | Value  | Units                  | Corresponding Elevation (ft msl) | Data Source  |
|--------------------|----------------|--------|------------------------|----------------------------------|--|
| Temperature        | Claimed as PBI | 135°   | Fahrenheit             | Claimed as P                     | Depth-dependent and based on a temperature gradient of 0.012° F/foot, as calculated from bottom hole temperature logged in wells in the study area with directional surveys, and a surface temperature of 72.5°F |
|                    | Claimed as PBI | 155°   |                        | Claimed as P                     |  |
|                    | Claimed as PBI | 177°   |                        | Claimed as P                     |  |
|                    | Claimed as PBI | 192°   |                        | Claimed as P                     |  |
| Formation Pressure | Claimed as PBI | 2,271  | Pounds per square inch | Claimed as P                     | Hydrostatic, assumed normal pressure aquifer   |
|                    | Claimed as PBI | 3,015  |                        | Claimed as P                     |  |
|                    | Claimed as PBI | 3,812  |                        | Claimed as P                     |  |
|                    | Claimed as PBI | 4,377  |                        | Claimed as P                     |  |
| Salinity           | Claimed as PBI | 20,700 | Parts per million      | Claimed as P                     | Attachment A, Section 2.8.2.3  |
|                    | Claimed as PBI | 20,700 |                        | Claimed as P                     | Attachment A, Section 2.8.2.4  |
|                    | Claimed as PBI | 20,700 |                        | Claimed as P                     | Attachment A, Section 2.8.2.5  |
|                    | Claimed as PBI | 21,100 |                        | Claimed as P                     | Attachment A, Section 2.8.2.6  |

**Table 3.4. Operational Details**

Claimed as PBI

**Table 3.5. Injection Pressure Details**

| Injection Pressure Details   | Claimed as PBI<br>[REDACTED] | [REDACTED] | [REDACTED] | [REDACTED] | [REDACTED] | [REDACTED] | [REDACTED] |
|--|------------------------------|------------|------------|------------|------------|------------|------------|
| Fracture gradient (psi/ft)   | 0.80                         | 0.80       | 0.80       | 0.80       | 0.80       | 0.80       | 0.80       |
| Maximum allowable downhole injection pressure (90% of fracture pressure) (psi) | 3,393                        | 3,245      | 3,304      | 5,957      | 5,697      | 5,833      | 6,674      |
| Elevation corresponding to maximum injection pressure (ft TVD)                 | 4,712                        | 4,507      | 4,589      | 8,274      | 7,913      | 8,102      | 9,269      |
| Elevation at the top of the perforated interval (ft TVD)                       | 4,712                        | 4,507      | 4,589      | 8,274      | 7,913      | 8,102      | 9,269      |
| Planned injection pressure (psi) / gradient (psi/ft) at top of perforations    | Claimed as PBI<br>[REDACTED] | [REDACTED] | [REDACTED] | [REDACTED] | [REDACTED] | [REDACTED] | [REDACTED] |

**Table 4.1. Simulation Sensitivity Scenarios**



Claimed as PBI

**Table 5.1. Wellbores in the AoR by Status**

| Status                | Count |
|-----------------------|-------|
| Active                | 0     |
| Idle                  | 0     |
| Plugged and Abandoned | 2     |
| Total                 | 2     |